OIL SPILL DETECTION BASED ON A SUPERPIXEL SEGMENTATION METHOD FOR SAR IMAGE

Ziyi Chen[1], Cheng Wang[1]*, Xiuhua Teng[2], Liujuan Cao[1], Jonathan Li[1, 3]

[1]Centre of Excellence for Remote Sensing and Spatial Informatics, School of Information Science and Engineering, Xiamen University, Xiamen, Fujian 361005, China
[2]School of Information Science and Engineering, Fujian University of Technology, Fuzhou, Fujian 350108, China
[3]Department of Geography and Environmental Management, University of Waterloo, Waterloo, Ontario N2L 3G1, Canada

Abstract

In this paper, a rapid oil spill detection approach which still maintains high detection accuracy is presented. The major contribution of the approach is using a superpixel segmentation method to subdivide the target SAR image into many approximate uniform scale pieces and preserves the boundaries well. Furthermore, a novel approach combine space distance, intensity deviation and size information together (SIS) is presented to eliminate the potential false positive, which is convenient and effective meanwhile. The proposed approach performs well and fast in both the synthetic data and RADARSAT-1 ScanSAR data which contain verified oil spills. The processing time is about 6s for a 512×512 image.

Index Terms—Oil spill detection, OTSU, SAR image, Superpixels

1. INTORDUCTION

Marine oil pollution, caused by discharge from ships, leakages from oil platforms, and oil-tanker accidents, is a major threat to fragile marine and coastal ecosystems[1]. To prevent the diffusion of oil spills in the first place, an efficient approach for geo-sensing and detection of oil spills is highly required to minimize its potential damages. In geo-sensing research, SAR is commonly used for ocean pollution monitoring due to the all-weather and all-day capabilities, great range and high resolution[2, 3]. Today, RADARSAT-1, RANDARSAT-2, ENVISAT, ERS-2, ALOS, TerraSAR-X and Cosmos skymed-1/2 are the main providers of satellite SAR images for oil spill monitoring. The observation is that the presence of an oil film on the sea surface can damp small waves due to the increased viscosity of the top layer, which will drastically reduce the measured backscattering energy and result in dark areas in SAR imagery[4, 5]. Generally speaking, three steps are taken for the oil spill detection: 1) dark-spot detection; 2) feature extraction; 3) oil spill classification[6, 7]. In the past few years, several efforts have been developed for automatic dark-spot detection or oil spill detection. A global threshold is widely used for dark-spot detection due to its computation efficiency. Representative approaches for the oil spill detection include, but not limited to, wavelets, fractal dimension estimation, marked point process, region merging, active contouring, SVM-based and neural networks based. However, most of the methods face the difficulty of balancing speed and robustness. On the other hand, the start points of most previous methods are based on pixels. Due to the speckle noise in SAR images, the intensity of pixels are inconsistent even in a smooth area, which make it difficult and unstable for classification based on pixels. Further more, the computation complexity of detection and classification based on pixels is usually high. Thus, superpixel is a new way to overcome the problems.

Recent years, superpixel based image segmentation has caused wide research attention, with many approaches developed. Representative approaches include graph-based algorithms and gradient-based algorithms. The latest achievements are Simple Linear Iterative Clustering (SLIC) [8], Edge-Weighted Centroidal Voronoi Tessellations-Based (VCells) [9] and Entropy-rate Clustering [10]. However, these approaches, although are fast, are either high computation complexity, low bondary recall, or not specifically designed for processing SAR oil spill images which contain speckle noise comparing to natural scene images.

In this paper, a rapid and high accurate oil spill detection method is proposed, which consists of a new superpixel generation approach that is suitable to SAR images. Then, based on segmented superpixels, Otsu [11] thresholding is applied to classify the SAR image into suspicious and determined false oil spills. In the last step, another contribution of this paper, the suspicious oil spill superpixels are clustered to eliminate the false positives. We then validate its efficiency via extensive experiments, reporting an average computation time about 6 seconds for oil spill detection with 512×512 image running on the MATLAB, with an 97.9% average segmentation accuracy in synthetic data and 96.8% in verified oil spill SAR images, respectively.

2. METHODOLOGY

Fig. 1 shows the flowchart of the proposed approach. The first and most critical step in the proposed method is the SAR image segmentation based on superpixel. The focus of the segmentation task is to precisely preserve the boundaries after fast segmentation while maintaining approximate uniform superpixel scale. We develop a novel superpixel segmentation algorithm to accomplish this task. In the second step, Otsu is applied for adaptive thresholding during image binaryzation. Finally, the suspicious superpixels are clustered, and then we eliminate the false positives

based on a novel approach called SIS which combines space distance, intensity deviation and size threshold together.

2.1 Superpixels Segmentation For SAR Image

The first stage of the proposed superpixel generation method is to uniformly partition the entire image into grids. In the second stage, the intensity centers and spatial centers of each partition are calculated. In the third stage, after the probability of x belonging to P_i is calculated, the pixel x is assigned to the partition with the largest probability. In the fourth stage, post processing is performed to deal with discontinuous superpixels.

Given a partition $P=\{P_i\}_{i=1}^{k}$ of image $I=\{g(x)\}_{x\in I}$ where $g(x)$ is the intensity of pixel x. The intensity center of each partition P_i is defined as

$$G_{P_i}=\frac{1}{|P_i|}\sum_{x\in P_i} g(x) \tag{1}$$

where $|P_i|$ is the number of pixels belonging to P_i.

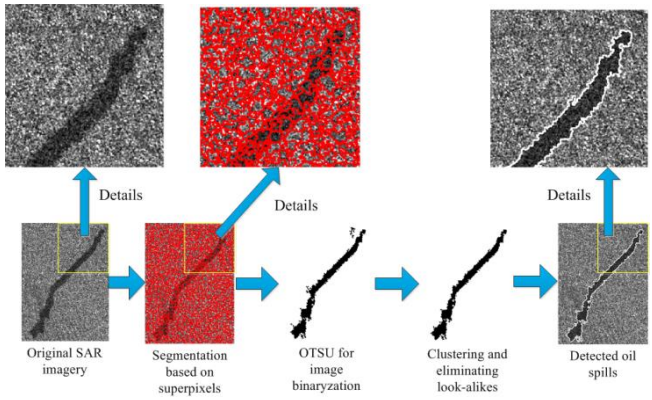

Fig. 1. Flowchart of the proposed approach. The images in the first row are the details of the images within the yellow rectangles in the second row.

And the spatial center is calculated as

$$S_{P_i}(m,n)=\left(\sum_{x\in P_i} w_x\cdot x_m,\sum_{x\in P_i} w_x\cdot x_n\right) \tag{2}$$

$$\hat{w}_x=\frac{G_{P_i}}{|g(x)-G_{P_i}|} \tag{3}$$

$$w_x=\frac{\hat{w}_x}{\sum_{x\in P_i}\hat{w}_x} \tag{4}$$

where w_x is the weight of pixel x, m and n are the position coordinates of x. Then, the probabilities of one pixel belonging to its neighbor superpixels are defined as

$$prob(x,P_i)=\frac{\sqrt{(\hat{g}(x)-G_{P_i})^2}}{A}\cdot\frac{\sqrt{(m-m_{P_i})^2+(n-n_{P_i})^2}}{B}\cdot\frac{N_{xi}}{8}$$
$$\hat{g}(x)=\frac{\sum_{i=-1}^{1}\sum_{j=-1}^{1} g(x_{m+i,n+j})}{9} \tag{5}$$

where A is a constant intensity value threshold, B is a constant space distance threshold, m_{P_i} and n_{P_i} are the space center coordinates of superpixel P_i, and N_{xi} is the number of 3×3 neighbors of x belonging to P_i.

After the superpixels are generated, the post processing checking for whether a superpixel is segmented into multiple disconnected parts is performed. The algorithm is summarized as follow:

Given: an image I and an arbitrary partition $\{P_i\}_{i=1}^{k}$

1: mark all pixels x and segments P_i as unvisited;
2: **for** all pixel $x\in I$ **do**
3: **if** x is unvisited **then**
4: mark x as visited and put x into queue q;
5: **if** P_i ($x\in P_i$) is unvisited **then**
6: mark P_i as visited;
7: **while** q is not empty
8: remove first element from q;
9: put first element's 3×3 neighbors belonging to P_i into q and mark them as visited;
10: **end while**
11: **end if**
12: **else if** P_i ($x\in P_i$) is visited **then**
13: put x into q, k=k+1;
14: **while** q is not empty
15: remove first element from q and reassign it to a new superpixel P_k;
16: put first element's 3×3 neighbors belonging to P_i into q and mark them as visited;
17: **end while**
18: update gray centers and space centers of P_i and P_k;
19: **end if**
20: **end for**

Return: $\{P_i\}_{i=1}^{k}$

After the disconnected superpixels are found, the disconnected parts will be reassigned to their neighbor connected superpixels with nearest gray scale distance, or the disconnected parts will form a new superpixel if their sizes are large enough.

2.2 SIS For Filtering Areas Of Look-Alikes

Since the image has been segmented by the superpixels, we apply Otsu for the image binaryzation based on the superpixels. Thus, the superpixels will be separated into confirmed negatives and suspicious ones. In order to filter the suspicious superpixels into confirmed positive ones, we combine space distance, intensity deviation and size information (SIS) together to eliminate the false suspicious superpixels. Before we utilize SIS, the suspicious superpixels are clustered into some disconnected suspicious parts. The parts which have larger size than the threshold M are considered as the centers (C) of the confirmed oil spills. Then, the space distance between one suspicious part and a center part is defined as:

$$Space\_Dist(C_c,C_i)=\min\{\sqrt{(m_x-m_y)^2+(n_x-n_y)^2},x\in C_c,y\in C_i\} \tag{6}$$

where x and y are pixels belonging to the center part C_c and suspicious part C_i, respectively. The parts with larger distance than N will be rejected as negatives. The intensity deviation is defined as:

$$Intensity\_Dist(C_i,C_c)=\sqrt{(I_{C_i}-I_{C_c})^2} \tag{7}$$

where I_{C_i} and I_{C_c} are the intensity of part C_i and center part C_c,

respectively. The clustered parts with larger intensity distance than the threshold N will be confirmed as negatives. Finally, a size threshold F is also used for eliminating the negatives, i.e. the parts with smaller size than the threshold will be eliminated.

3. EXPERIMENTAL RESULTS

In order to verify the efficiency and effectiveness of the proposed method, both synthetic data and real SAR image data are used, the latter of which was captured by the RADARSAT-1 satellite sensor located at the west coast of Canada (near to Newfoundland) with an HH polarization. The spatial resolution of the SAR intensity images was 50 m. During the tests, the parameters of the proposed method were tuned for best performance. The initialize size of the superpixels during the tests was 200 pixels except detections for linear oil spills. Parameters iteration time in superpixel algorithm was set at 10, the A and B in Eq. (5) were set at10 and 60 respectively, and the M, N, and F in section 2.2 were tuned according to the actual oil spill regions in SAR imagery. All detections were running on the MATLAB, and all experiments were conducted on a computer with an Intel Core i5 3.1GHz processor and a 4 GB RAM.

3.1 Evaluation Protocols

The following three evaluation criteria are used for evaluating the accuracy of the proposed oil spill detection algorithm: commission error, omission error and synthetic detection accuracy. Fig. 2 illustrates the commission areas and omission areas. Commission is the detected area outside the ground truth, and the commission error is defined as:

$$CE = \frac{N_c}{N_c + N_o + N_{correct}} \tag{8}$$

where N_c and N_o are the pixel numbers of the commission areas and omission areas, respectively. $N_{correct}$ is the pixel number of the correct detection areas. Similarly, omission is the ground truth area outside the detection result, and omission error is defined as:

$$OE = \frac{N_o}{N_c + N_o + N_{correct}} \tag{9}$$

, and the synthetic detection accuracy (SDA) is defined as:

$$SDA = \frac{N_{correct}}{N_c + N_o + N_{correct}} \tag{10}$$

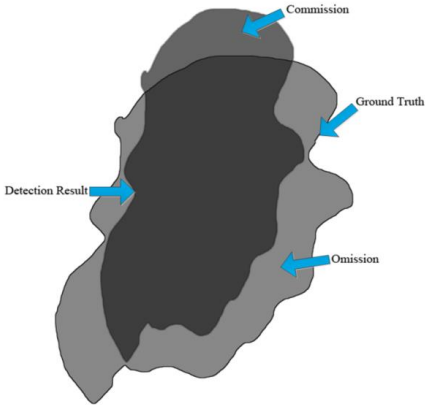

Fig. 2. Illustration of the commission and omission errors. The ground truth is defined as the area inside the black line. The darker areas are the detection result, and the darkest area is the overlap of detection result and ground truth.

3.2 Tests In Synthetic Data

In this part, we test the proposed method in several synthetic oil spill images with the MATLAB. Different degrees of noises are added into the synthetic images. Fig. 3 shows several detection examples of synthetic oil spills with different speckle noise levels, and Fig. 4 shows the SDA during the tests in the synthetic images. The curve shows that the SDA of our proposed method reached as high as 99.9% when the speckle noise degree is lower than 5.0. Moreover, the accuracy of SDA is still higher than 97% when the speckle noise level was 50.0.

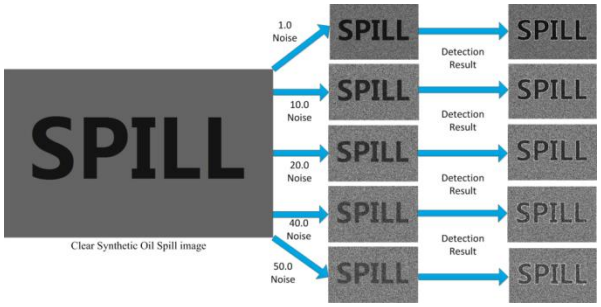

Fig. 3. Detections in synthetic data

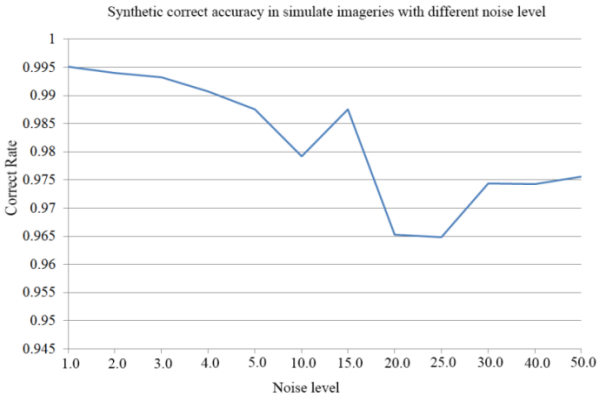

Fig. 4. Synthetic detection accuracy (SDA) in synthetic oil spills with different noise levels.

3.3 Detection In Real SAR Images

In this part, we test our proposed method on real SAR images with different anomalies, including the following: well-defined versus not well-defined, linear versus massive, homogeneous versus heterogeneous backgrounds. Fig. 5 shows some examples of the detections in real SAR images.

In order to analyze in depth, we show the Table 1 which gives the detection details during the test: Clearly, there is little difference among the detection accuracies for the different types of anomalies, which proves the robustness of the proposed method when detecting for different types of oil spills. And the mean average detection accuracy ranges from 96.32% to 97.24%. The worst performance among the tests is 91.84%. On the other hand, both the commission and omission errors of all types of anomalies are very low. Also, in the worst cases, the commission error is 6.48% and the omission error is 4.6%, respectively.

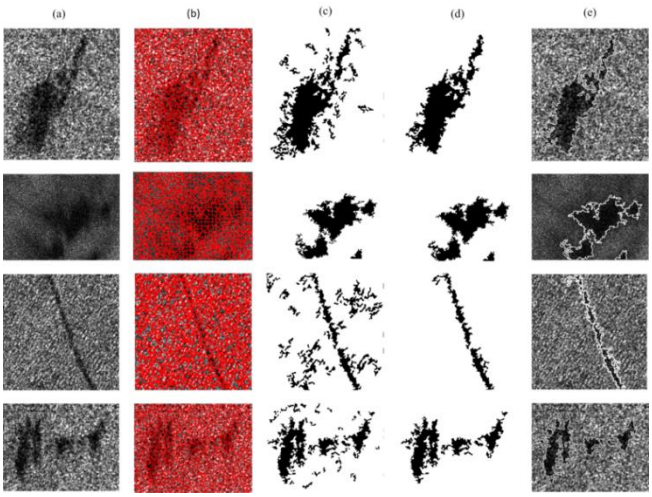

Fig. 5. Examples of oil spill detections in SAR images. (a). Original SAR images. (b). Segmentations by the proposed superpixel method. (c). Binaryzation results by OTSU thresholding. (d). Results after filtering look-alikes. (e). Final results detected by the proposed method.

Table 1 Mean values of the accuracies achieved by the proposed method for different types of anomalies.

	CE	OE	SDA	Test time
Well-defined	0.0235	0.0107	0.9658	10
Not well-defined	0.0036	0.0264	0.97	7
Linear	0.0122	0.0187	0.9691	10
Massive	0.0197	0.015	0.9653	7
Homogeneous	0.011	0.0166	0.9724	8
Heterogeneous	0.0192	0.0176	0.9632	9

4. Conclusion

In this paper, a rapid, highly accurate, and robust oil spill detection method is proposed. Our first contribution is an efficient superpixel segmentation approach designed for SAR images with special consideration of preserving boundaries while maintain approximate uniform superpixel scale. Our second contribution, a simple and effective principle SIS, instead of classic classification methods with high computation complexity, is proposed to eliminate the false positives.

To verify the performance of the proposed method, the synthetic and real SAR data are both tested by the proposed method. In synthetic data, the averages of detection accuracy, omission error, and commission error among different speckle noise levels were 97.9%, 0.9% and 1.2%, respectively. In real SAR images, the average of detection accuracy, omission error and commission error were 96.8%, 1.7% and 2.1%, respectively. Regardless of the type of the anomaly in the SAR imagery, including extreme scenarios, the proposed method attains high detection accuracy and low commission and omission errors, thereby proving the proposed method is highly efficient, effective and robust. In terms of speed, the proposed method requires only about 6 seconds to process a 512×512 image running on the MATLAB, which is faster than the existing fastest method in the literature.

5. Acknowledgement

This work was supported in part by the National Natural Science Foundation of China (Grant No. 61371144) and the Natural Sciences and Engineering Research Council of Canada (NSERC) (Grant No. 111368).

6. References

[1] Y. Shu, J. Li, H. Yousif, and G. Gomes, "Dark-spot detection from SAR intensity imagery with spatial density thresholding for oil-spill monitoring," *Remote Sensing of Environment,* vol. 114, pp. 2026-2035, 2010.

[2] C. Brekke and A. H. Solberg, "Oil spill detection by satellite remote sensing," *Remote Sensing of Environment,* vol. 95, pp. 1-13, 2005.

[3] M. F. Fingas and C. E. Brown, "Review of oil spill remote sensing," *Spill Science & Technology Bulletin,* vol. 4, pp. 199-208, 1997.

[4] W. Alpers and H. Hühnerfuss, "Radar signatures of oil films floating on the sea surface and the Marangoni effect," *Journal of Geophysical Research: Oceans (1978–2012),* vol. 93, pp. 3642-3648, 1988.

[5] P. Trivero, B. Fiscella, F. Gomez, and P. Pavese, "SAR detection and characterization of sea surface slicks," *International Journal of Remote Sensing,* vol. 19, pp. 543-548, 1998.

[6] A. Taravat, D. Latini, and F. Del Frate, "Fully Automatic Dark-Spot Detection From SAR Imagery With the Combination of Nonadaptive Weibull Multiplicative Model and Pulse-Coupled Neural Networks."

[7] F. Del Frate, A. Petrocchi, J. Lichtenegger, and G. Calabresi, "Neural networks for oil spill detection using ERS-SAR data," *Geoscience and Remote Sensing, IEEE Transactions on,* vol. 38, pp. 2282-2287, 2000.

[8] R. Achanta, A. Shaji, K. Smith, A. Lucchi, P. Fua, and S. Susstrunk, "SLIC superpixels compared to state-of-the-art superpixel methods," 2012.

[9] J. Wang and X. Wang, "VCells: Simple and efficient superpixels using edge-weighted centroidal Voronoi tessellations," *Pattern Analysis and Machine Intelligence, IEEE Transactions on,* vol. 34, pp. 1241-1247, 2012.

[10] M.-Y. Liu, R. Chellappa, O. Tuzel, and S. Ramalingam, "Entropy-Rate Clustering: Cluster Analysis via Maximizing a Submodular Function subject to a Matroid Constraint," *IEEE Transactions on Pattern Analysis and Machine Intelligence,* p. 1, 2013.

[11] N. Otsu, "A threshold selection method from gray-level histograms," *Automatica,* vol. 11, pp. 23-27, 1975.